Research Square

Preprints are preliminary reports that have not undergone peer review.
They should not be considered conclusive, used to inform clinical practice,
or referenced by the media as validated information.

Hydrochemical components evolution and suitability assessment of groundwater in Emei-Jiajiang Plain of Southwestern China

Hao Liu
Sichuan Institute of Land and Space Ecological Restoration and Geological Hazard Prevention
Xin Huang
Sichuan Institute of Land and Space Ecological Restoration and Geological Hazard Prevention
anbang huang
Institute of Exploration Technology, Chinese Academy of Geological Sciences
jibo shi
Sichuan Institute of Land and Space Ecological Restoration and Geological Hazard Prevention
yanming liu
sxffzyszys@163.com

China Institute of Geological Environmental Monitoring
peng zhang
Sichuan Institute of Land Science and Technology (Sichan Center of Satellite Application Technology)

Research Article

Keywords: groundwater, hydrochemistry, ion ratio, genetic analysis, APCS-MLR, PMF, health risk assessment, irrigation suitability

Posted Date: April 1st, 2026

DOI: https://doi.org/10.21203/rs.3.rs-8840552/v1

License: This work is licensed under a Creative Commons Attribution 4.0 International License.
Read Full License

Additional Declarations: No competing interests reported.

Hydrochemical components evolution and suitability assessment of groundwater in Emei-Jiajiang Plain of Southwestern China

Hao Liu[1], Xin Huang[1], Anbang Huang[2], Jibo Shi[1], Yanming Liu[3]*, Peng Zhang[4]*,

1.Sichuan Institute of Land and Space Ecological Restoration and Geological Hazard Prevention, Chengdu , 610081, China; 970852963@qq.com(H.L.); cughx2014@163.com(X.H.);1669031874@qq.com(J.B.S.)

2.Institute of Exploration Technology, Chinese Academy of Geological Sciences, Chengdu , 611734, China; 362641894@qq.com;

3.China Institute of Geo-Environmental Monitoring , Beijing , 10081, China; sxffzyszys@163.com;

4.Sichuan Institute of Land Science and Technology (Sichuan Center of Satellite Application Technology), Chengdu 610045, China;mariogomez@qq.com

*Correspondence: sxffzyszys@163.com; mariogomez@qq.com

Abstract:To investigate the hydrochemical formation mechanisms of groundwater in Emei-Jiajiang Plain and to analyze the sources of hydrochemical components, traditional hydrochemical diagram methods, mathematical statistics, the Absolute Principal Component Scores-Multiple Linear Regression model (APCS-MLR), and the Positive Matrix Factorization model (PMF) were used. Based on the inorganic component contents of 19 Quaternary groundwater samples, the hydrochemical characteristics of Quaternary groundwater, the contribution rates of hydrochemical component sources, and water quality status were analyzed. The results show that: The hydrochemical composition of groundwater is mainly controlled by rock weathering, with carbonates and silicates being important sources of groundwater ionic components, and the dissolution of carbonate is comprehensively controlled by H_2CO_3 and H_2SO_4. Human activities have exerted a certain impact on the groundwater in the study area, mainly from domestic sewage and agricultural sewage. Both the APCS-MLR and PMF results indicate that natural sources, mixed sources from of industrial and agricultural activities, agricultural activities, and domestic sewage are the main factors affecting the groundwater in the study area. The groundwater quality in the study area is generally good. Entropy Weight Water Quality Index (EWQI) evaluation results show that most areas are suitable for direct human consumption, with a low potential non-carcinogenic risks, and suitable for irrigation, only local sites have health risks and are not suitable for irrigation.

Keywords: groundwater; hydrochemistry; ion ratio; genetic analysis; APCS-MLR; PMF; health risk assessment; irrigation suitability

Introduction

As a crucial strategic resource in China, groundwater supplies 70% of domestic drinking water and 40% of industrial and agricultural water use, making it indispensable for national survival and economic development (Shrestha S et al., 2016; Zhai Y et al., 2019). The chemical composition of groundwater is primarily influenced by natural factors such as topography, lithology, groundwater recharge-runoff-discharge conditions and climate (Chin et al., 2019; Cui et al., 2012). However,

with economic development and rapid urbanization, human activities-including land-use changes, industrial operations, and agricultural practices-have significantly disrupted the natural evolution of groundwater systems. The unregulated discharge of domestic wastewater and excessive application of nitrogenous fertilizers have led to the exceedance of permissible limits for Inorganic nitrogen (Du et al., 2018; Zhang et al., 2019). In severe cases, this can induce illnesses such as gastritis, methemoglobinemia, and blue baby syndrome, posing serious risks to human health (Lv et al., 2019; Chen et al., 2020). Furthermore, poor-quality groundwater may also degrade soil quality and inhibit crop growth (Zhu et al., 2021; Tang et al., 2019).

Scholars worldwide commonly employ methods such as ion ratios, hydrochemical diagrams, statistical analysis, environmental isotopes, and hydrogeochemical modeling to study the hydrochemical evolution of groundwater in urbanized areas. Groundwater quality assessment is often conducted using approaches like the single-factor index method (Ministry of Ecology and Environment & Standardization Administration, 2017), the Entropy Weighted Water Quality Index (EWQI)(Zhang et al., 2010), and comprehensive water quality index methods (Liu et al., 2013; Xu and Xu, 2001). Additionally, receptor models such as the Absolute Principal Component Scores-Multiple Linear Regression model (APCS-MLR) and the Positive Matrix Factorization model (PMF) are applied to quantitatively apportion the contributions of natural and anthropogenic sources to specific hydrochemical indicators (Paatero and Tapper, 2014; Thurston and Spengler, 1987; Lu et al., 2010), thereby supporting the scientific management of water resources.

Emei-Jiajiang Plain is located in the Sichuan Basin of southwestern China, which is the most economically dynamic and densely populated region of Sichuan Province, and serves as a pivotal area for establishing a higher-standard "Tianfu Granary". This study aims to analyze the hydrochemical characteristics of groundwater and identify the factors dominating hydrochemistry in Emei-Jiajiang Plain, And applies the APCS-MLR and PMF models to trace the sources of groundwater chemical indicators. Additionally, this study will use EWQI to assess groundwater quality, and evaluate the quality of groundwater for drinking purposes and health risk analysis, and assess the suitability of groundwater for agricultural irrigation by utilizing the basic irrigation index. The findings will deepen the understanding of groundwater chemical evolution, water environment, and water quality in the region, thereby providing a scientific basis for the protection and sustainable utilization of groundwater resources in the study area.

1 Study Area

Emei-Jiajiang Plain is composed of Emei Plain and Jiajiang Plain(Figure.1 a,b), and borders the Western Sichuan Plain to the northeast and extends toward the Ebian Yi Autonomous County to the southwest. The average elevation ranges between approximately 400~500 m. The region experiences a subtropical humid monsoon climate, with an average annual temperature of around 17°C. Seasons are distinct, featuring warm winters and hot summers. Annual precipitation averages about 1300 mm, with rainfall heavily concentrated from May to September, accounting for 78.5% of the yearly total.

Emei-Jiajiang Plain, situated along both sides of the Minjiang River, Qingyijiang River and Dadu River, features well-developed alluvial deposits that form extensive floodplains. The Quaternary strata in the area are primarily composed of Holocene fluvial deposits, Pleistocene glacial and glaciofluvial accumulations, as well as Tertiary fluvio-lacustrine sedimentary layers, with Tertiary strata exclusively distributed in the Emei Plain. Bedrock fissure water mainly exists as shallow weathered fissure aquifers, occurring at relatively shallow depths and predominantly distributed in hilly regions. Porous-fissure water in clastic rocks generally manifests as confined groundwater, characterized by relatively thick aquitards.

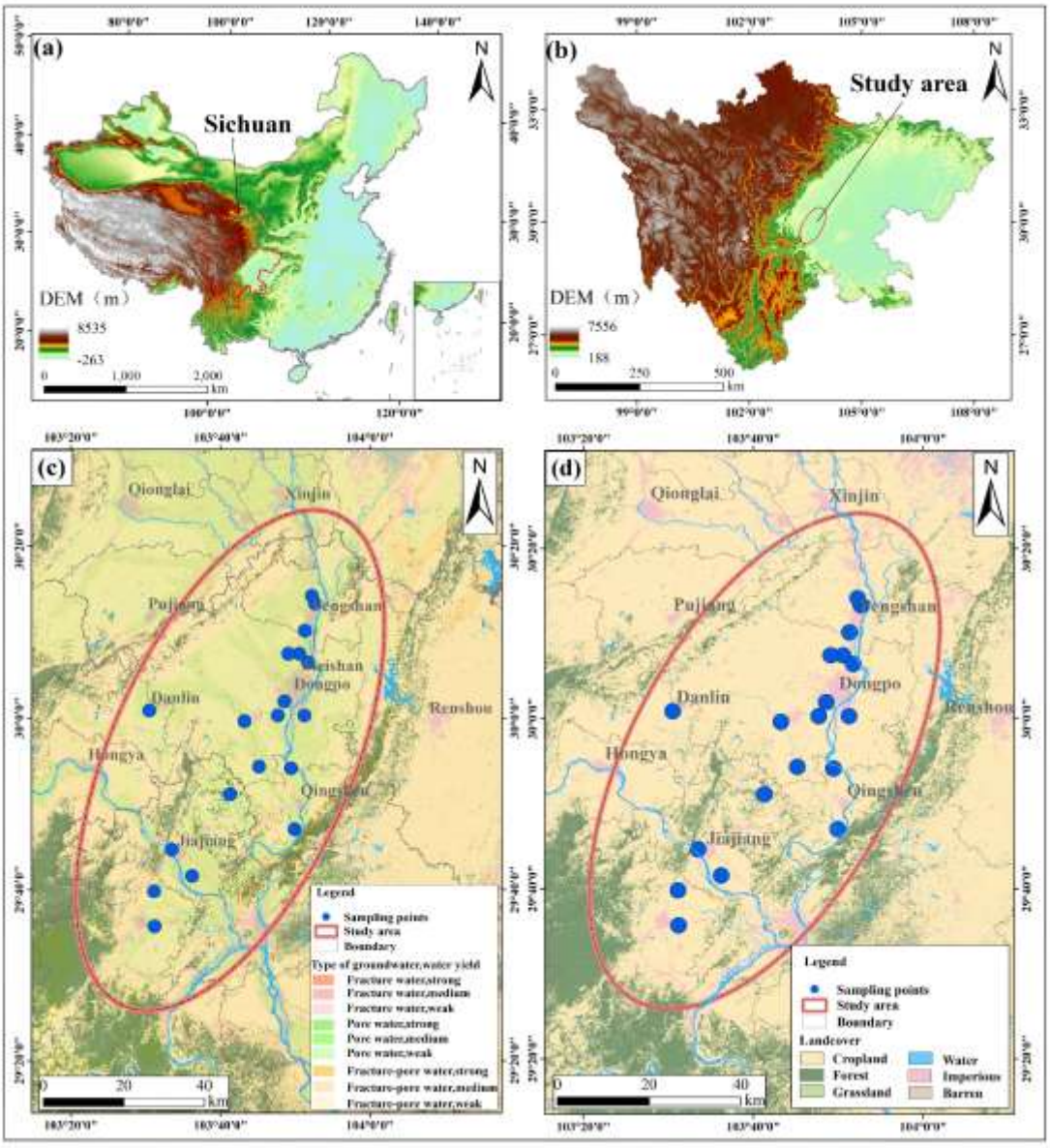


Figure.1 Overview of the study area. (a,b) indicate the relative location of the study area. (c,d) provide the hydrogeological conditions and landuse of the area, while display the distribution of the 19 sampling sites.

As shown in Figure.1 c,d, within the Jiajiang Plain, the downstream sections of the Minjiang, Dadu, and Qingyi Rivers, emerging from the Qianfoyan valley, exhibit relatively stable groundwater

tables in the floodplains and first terraces distributed in strip-like patterns along both banks. The water table depth ranges from 1~6m, with abundant groundwater resources, and these aquifers are composed of $Q_{4\text{-}1}^{al}$, $Q_{4\text{-}2}^{al+pl}$. The upper layer generally consists of 0.5~2m of clayey sand or muddy silt, while the lower layer primarily comprises variably thick gravel and pebbles with good roundness, grain sizes of 2~15cm, thicknesses ranging from 0 to 10m, and a maximum thickness of 20m. Areas with relatively high groundwater yield are mainly distributed along the second terraces on both banks of the Minjiang River and the upstream section of the Qingyi River east of Qianfoyan. Within the Minjiang River basin, the floodplains and first terraces on the right bank exhibit better water yield and cover a larger area. Porous phreatic water in the Emei Plain is formed by Holocene and Pleistocene deposits, exhibiting local semi-confined conditions, and is primarily distributed across the floodplain terraces of the Emei Plain. Regions with abundant groundwater resources are composed of $Q_{4\text{-}1}^{al}$, $Q_{4\text{-}2}^{al+pl}$, with an upper layer of 0.5~2m of clayey sand or clayey silt, underlain by 0~10m of gravel and pebbles(Zhou, 1981; Li, 2021).

2 Data and Methods

2.1 Sample Collection and Analysis

A total of 19 groundwater samples are collected from national groundwater monitoring stations located within Emei-Jiajiang Plain, and all sampling points are long-term, closed professional groundwater monitoring stations with well depths of approximately 25m. The water sampling processes adhere to the DZ/T 0307-2023 *Specification for Operation and Maintenance of Groundwater Monitoring Networks*. Prior to sampling, prolonged pumping and well purging are conducted until on-site water quality parameters (pH, conductivity, dissolved oxygen, and redox potential) meet the technical specification requirements.

32 hydrochemical indicators are analyzed accordancing with to the GB/T 14848-2017 *Groundwater Quality Standard* for each sample: pH, total hardness (TH), total dissolved solids (TDS), Ca^{2+}, Na^{+}, Mg^{2+}, K^{+}, HCO_3^{-}, CO_3^{2-}, SO_4^{2-}, Cl^{-}, total iron (TFe), Mn^{2+}, Cu^{2+}, Zn^{2+}, Al^{2+}, volatile phenolic compounds (VOC-Ph), linear alkylbenzene sulfonates (LAS), chemical oxygen demand (COD), S^{2-}, NO_3^{-}-N, NO_2^{-}-N, NH_4^{+}-N, CN, F^{-}, I^{-}, Hg^{2+}, As^{3+}, Se^{4+}, Cd^{2+}, Cr^{6+} and Pb^{2+}. The analyses are performed using ion chromatography system (ICS-600), atomic absorption spectrophotometer (ZA3000), and inductively coupled plasma mass spectrometer (iCAP RQ).The measured values of NO_3^{-}-N, NO_2^{-}-N, NH_4^{+}-N contamination are expressed as nitrogen concentrations.

2.2 Principal Research Methods

2.2.1 Positive Matrix Factorization (PMF)

The Positive Matrix Factorization (PMF) model, proposed by Paatero and Tapper (1994), is a receptor modeling technique based on a weighted least squares algorithm. It iteratively decomposes a data matrix to obtain optimal factor matrices (G and F), with the objective function minimized through the iterative process.

2.2.2 Absolute Principal Component Score-Multiple Linear Regression (APCS-MLR)

The Absolute Principal Component Score-Multiple Linear Regression (APCS-MLR) receptor model builds upon Principal Component Analysis (PCA). After obtaining the rotated factor loading matrix and eigenvectors from PCA, the model performs multiple linear regression between the Absolute Principal Component Scores (APCS)-derived from the eigenvectors and standardized data and the measured concentrations. This regression quantifies the contribution rate of each source factor to individual water quality indicators. The validity of the source apportionment results is evaluated by linearly fitting the predicted concentrations from the regression model against the measured concentrations (Thurston and Spengler, 1987; Lu et al., 2010).

2.2.3 Entropy Weighted Water Quality Index (EWQI)

The Entropy Weighted Water Quality Index (EWQI) method assesses groundwater quality by assigning weights to water quality indicators based on information entropy, providing a comprehensive reflection of overall water quality. It has been widely applied in relevant studies (Zhang et al., 2010). The main procedure involves constructing the initial water quality data matrix, normalizing the data (with pH treated as a moderate-type indicator), calculating the information entropy and entropy weight for each indicator, computing the final EWQI value, and classifying water quality into five categories (Liu et al., 2024). The classification criteria is shown in Table 1.

Table 1. Groundwater quality classification criteria based on EWQI value

EWQI value	Classification	Water quality
≤50	I	Excellent
50~100	II	Good
100~150	III	Medium
150~200	IV	Poor
>200	V	Extremely poor

2.2.4 Human Health Risk Assessment (HHRA)

Contaminated water threaten human health through multiple pathways, such as drinking ingestion and dermal contact, therefore health risk assessment is crucial for water quality evaluation and management. The HHRA model developed by the United States Environmental Protection Agency (USEPA), which quantifies potential health risks, has become an essential tool for assessing the relationship between water quality and human health risks (USEPA, 2004). Due to physiological differences between adults and children, health risk assessments should be conducted separately for each group (Gao, 2020). The relevant parameters are presented in Table 2 (Zhang et al., 2019; Xu and Zhang, 2018). The Health Indices (HI) uses a reference threshold of 1, which HI < 1 indicates the risk is within an acceptable (controllable) range, and HI > 1 signifies an unacceptable (uncontrollable) risk. In the latter case, groundwater quality warrants attention, and necessary measures should be implemented.

Table 2. Parameters of health risk model

Group	Oral						Der			
	IR	BW	EF	ED	$AT_{non\text{-}carcinogenic}$	$AT_{carcinogenic}$	SA	EV	K_p	t_{event}
Aldults	1.5	61.75	365	30	ED*365	74.68*365	16110	1	0.001	0.25
Children	0.85	15	365	6	ED*365	10*365	8650	1	0.001	0.33

Note:IR (L/ D), intake rate; BW (kg), body weight; EF (d/a), annual exposure frequency; ED (a), exposure duration; AT (d), saverage time; SA (cm^2), surface area; EV (d^{-1}) , exposure numbers of events; Kp (cm/h), skin permeability ;t_{event}(h) , duration of skin contact.

2.2.5 Irrigation Suitability Assessment

Hydrochemical parameters of groundwater are crucial factors influencing its suitability for irrigation (Esmaeili-Vardanjani M et al., 2015; K H B, 1969; Richards , 1954), to ensure a comprehensive evaluation of irrigation water quality, this study specifically selected six indicators such as Sodium Percentage (Na%), Sodium Adsorption Ratio (SAR), Magnesium Hazard (MH), Permeability Index (PI), Soluble Sodium Percentage (SC) and Residual Sodium Carbonate (RSC) to fully interpret and evaluate the chemical properties of the water.

If water contains high levels of sodium, it can react with carbonates and cause soil alkalinity to rise. Additionally, excessive amounts of sodium chloride can lead to soil salinization, which decreases soil permeability and hinders water flow through the soil, ultimately affecting crop growth (Na et al. 2020; Bishwakarma et al., 2009). The formulas for calculating Na^+ , SC are presented in Equation (1), (2).

$$Na\% = N(Na^+)/(N(Na^+)+N(Ca^{2+})+N(Mg^{2+})+N(K^+))\times 100\% \quad (1)$$

$$SC = (N(Na^+)++N(K^+))/(N(Na^+)+N(Ca^{2+})+N(Mg^{2+})+N(K^+))\times 100\% \quad (2)$$

The SAR is an important measure of the concentration of Na^+in groundwater. A higher SAR value indicates a greater adsorption effect on Na^+, which can displace Ca^{2+} and Mg^{2+}, impeding soil aeration and hindering root respiration and growth (Arumugam and Elangovan, 2009; Todd et al., 1980). High concentration of Mg^{2+} can induce magnesium alkalization in soil, negatively affecting soil structure and causing toxicity to crops. The formula for SAR values is shown in Equation (3).

$$SAR = N(Na^+)/\sqrt{1/2(N(Ca^{2+})+N(Mg^{2+}))} \quad (3)$$

High concentration of Mg^{2+} can induce magnesium alkalization in soil, negatively affecting soil structure and causing toxicity to crops (Bian et al., 2018).The formula for MH values is shown in Equation (4).

$$MH = N(Mg^{2+})/N(Ca^{2+})+N(Mg^{2+}) \quad (4)$$

The PI parameter can be utilized to evaluate if groundwater is appropriate for irrigation and it is determined by specific ions, such as calcium, magnesium, sodium, and bicarbonate ions (Doneen, 1964). Prolonged use of irrigation water may alter soil permeability, this reduction in soil permeability can negatively affect the absorption of nutrients and crop growth. The formula for PI is shown in Equation (5).

$$PI = (N(Na^+)+\sqrt{N(HCO_3^-)})/(N(Na^+)+N(Ca^{2+})+N(Mg^{2+})) \quad (5)$$

The suitability of irrigation water quality is evaluated based on the RSC parameter, which indicates the relationship between weak acids and alkaline earth minerals present in groundwater (Eaton and Frank, 1950). High RSC values in irrigation water can negatively impact crop yields and cause severe alkali damage if used for prolonged periods.The formula for RSC is shown in Equation

(6).

$$RSC = N(HCO_3^-) - N(Mg^{2+}) - N(Ca^{2+}) \quad (6)$$

The ion units involved in the above formula are all meq/L.

3 Results and Discussion

3.1 Hydrochemical Characteristics

The study area exhibited the values of pH ranged from 6.33 to 7.71, with an average of 7.04, indicating a predominantly neutral condition. The total dissolved solids (TDS) ranged from 125~1040 mg/L, with an average 525.05 mg/L. The major cations were Ca^{2+}, Na^+, Mg^{2+} and K^+, with their average mass concentrations (ρ) following the order: ρ (Ca^{2+}) (117.54 mg/L) > ρ (Na^+) (28.86 mg/L) > ρ (Mg^{2+}) (19.32 mg/L) > ρ (K^+) (4.61 mg/L). The concentrations of Ca^{2+} ranged from 21.4~261 mg/L. Among anions, HCO_3^- is dominant, with concentrations between 99.2~459.4 mg/L ,with an average of 307.03 mg/L.According to the Class Ⅲ water standards specified in the GB/T 14848-2017 *Groundwater Quality Standard*, the main indicators with exceedance rates were Mn^{2+} (73.68%), total hardness (TH) (31.58%). Exceedances were also observed for SO_4^{2-} (10.53%), TDS (5.26%), pH (5.26%), and NO_3^--N (5.26%).The predominant hydrochemical type of groundwater was Ca-HCO_3.The findings are presented in both Table 3 and Figure 2.

Table 3. Main hydrogeochemical parameters

Indicator	Maximum	Minimum	Average	Median	Standard deviation	Coefficient of variation	Over-standard rate
TH	818	82	382.47	398.00	184.72	0.48	31.58
TDS	1040	125	525.05	526.00	226.54	0.43	5.26
pH	7.71	6.33	7.04	6.99	0.26	0.04	5.26
K^+	29.3	0.68	4.61	2.51	6.57	1.43	-
Na^+	69.6	8.27	28.86	26.10	16.77	0.58	-
Mg^{2+}	38.1	5.59	19.32	20.80	8.23	0.43	-
Ca^{2+}	261	21.4	117.54	121.00	62.38	0.53	-
SO_4^{2-}	404	17.8	125.67	103.00	93.39	0.74	10.53
Cl^-	162	2.72	40.14	31.80	36.89	0.92	0.00
HCO_3^-	459.4	99.2	307.03	336.90	114.43	0.37	-
CO_3^-	\	\	\	\	\	\	-
Mn^{2+}	0.77	\	0.35	0.43	0.25	0.72	73.68
NO_3^--N	54.6	0.055	5.07	0.27	12.49	2.46	5.26
NO_2^--N	\	\	\	\	\	\	0.00
NH_4^+-N	0.37	0.02	0.10	0.07	0.11	1.12	0.00

Note: Over-standard rates units are %; except for pH (dimensionless), all indicator units are mg/L; "\" indicates that the content is below the detection limit; " – " indicates that the standard for this indicator is not specified in the GB/T 14848-2017 *Groundwater Quality Standard*.

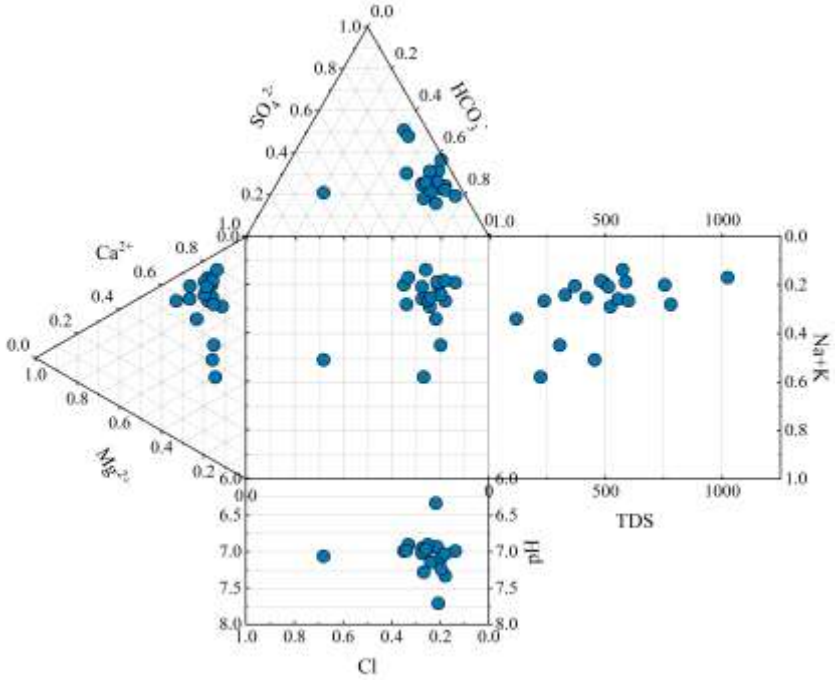


Figure.2 Hydrochemical Durov diagram of groundwater

3.2 Hydrochemical Genetic Classification

The Pearson correlation coefficient method was used to analyze the relationships among the major hydrochemical indicators in the study area. As shown in Figure 3, significant correlations (0.76~0.97) were observed among TDS, TDS, Ca^{2+}, Mg^{2+}, HCO_3^- and SO_4^{2-}, which are attributed to water-rock interactions, typically originating from the dissolution of calcite ($CaCO_3$), dolomite ($CaMg(CO_3)_2$), and gypsum ($CaSO_4$) within the region. A moderate correlation (0.41) was found between NH_4^+ and Mn^{2+}, likely due to the generally semi-closed reducing environment in the study area, which promotes the reductive dissolution of overlying nitrogen-rich organic silt layers and iron-manganese nodules, leading to concurrent increases in NH_4^+ and Mn^{2+} concentrations. Overall, water-rock interactions exert a significant influence on the hydrochemical evolution of groundwater in the area.



Figure.3 Correlation analysis results

3.3 Ion Source Analysis

The Gibbs diagram is a useful tool for understanding the correlation between aquifer lithology and water composition. As shown in Figure4 a,b, Gibbs diagrams indicate that almost all sampling points in the study area fall within the rock domainance area, suggesting that water-rock interaction is the primary factor contributing to the formation of groundwater chemistry in the study area (Gibbs, 2015). Additionally, one sample point is located in the central-right section of the Gibbs diagram, with moderate ρ (TDS) (approximately 300 mg/L, content, the same below), ρ (Na^+)/ ρ (Na^++Ca^{2+}) ratio of about 0.5, and ρ (Cl^-)/ ρ (Cl^-+HCO_3^-) ratio close to 0.75, which implies potential influence from anthropogenic activities, leading to external inputs of Na^+ and Cl^-.

For groundwater predominantly controlled by water-rock, ion ratio relationships can reflect the characteristics of hydrochemical formation and evolution. Ratios such as $c(Ca^{2+})/c(Na^+)$, $c(HCO_3^-)/c(Na^+)$, and $c(Mg^{2+})/c(HCO_3^-)$ (molar ratio, the same below)are used to further clarify the specific mineral dissolution processes controlling groundwater chemistry (Gaillardet et al., 1999). As shown in Figure 4c,d, the sample points are mainly distributed between silicates and carbonates end-members, indicating that carbonates and silicates are key factors controlling the hydrochemistry of the unconsolidated porous aquifer in the study area. The silicates influence is associated with the widely distributed Quaternary gravel layers, while the contribution from evaporite mineral dissolution is negligible.

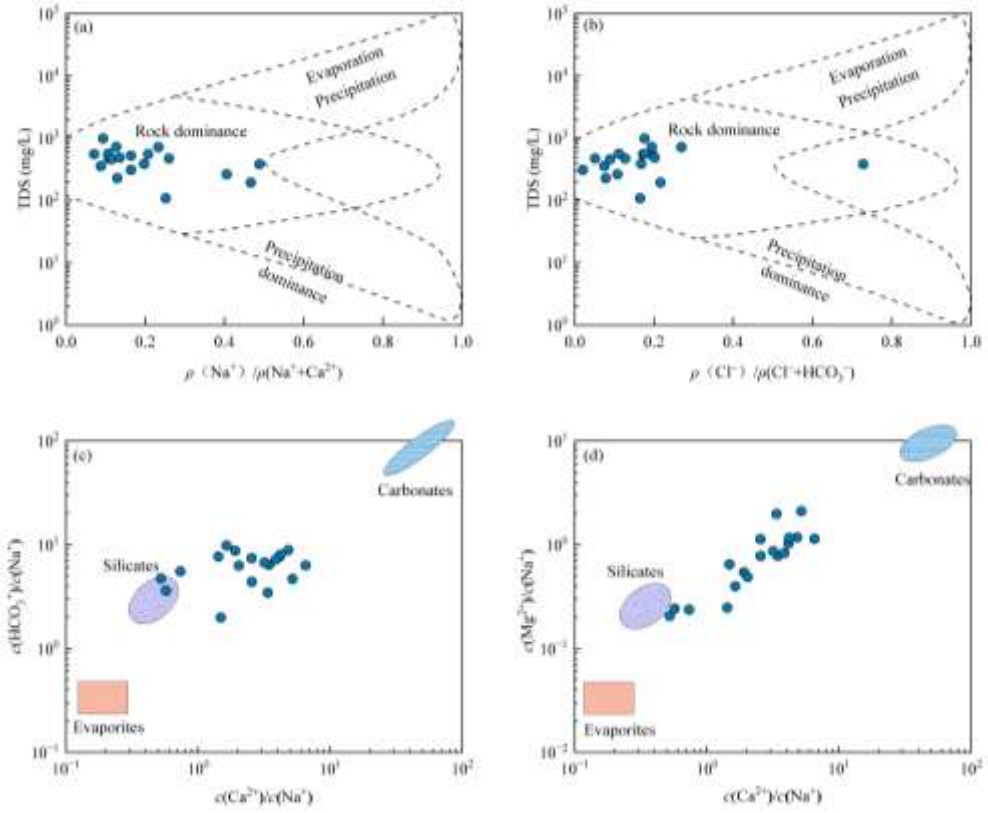


Figure.4 End-member diagram of groundwater

The proportion of major ions present in groundwater can be a valuable technique for detecting potential water-rock interactions within groundwater systems, Figure 5a shows that most ions of

$N(SO_4^{2-}+Cl^-)$ and $N(HCO_3^-)$(milliequivalent, the same below) exceed 1, which indicates that carbonate (e.g., calcite, dolomite) are a significant source of ions in the groundwater (Zhang et al., 2020). As shown in Figure 5b, the ratio of $N(HCO_3^-+SO_4^-)$and $N(Ca^{2+}+Mg^{2+})$will be equivalent to 1, suggesting silicates is also an important source.

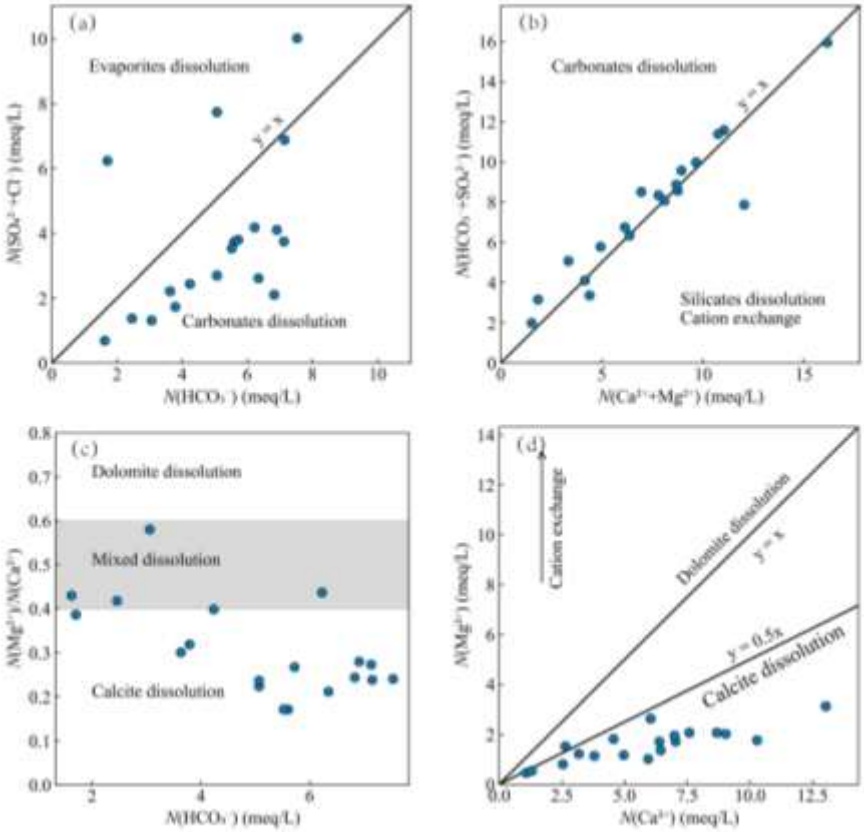


Figure.5 Scatter plots of (a) $N(SO_4^{2-}+Cl^-)$ VS. $N(HCO_3^-)$; (b)$N(Ca^{2+}+Mg^{2+})$ VS. $N(HCO_3^-+SO_4^{2-})$; (c) $N(Ca^{2+})/N(Mg^{2+})$ VS. $N(HCO_3^-)$; (d) $N(Mg^{2+})$ VS. $N(Ca^{2+})$

The primary minerals of carbonate are calcite and dolomite and the ratio of $N(Mg^{2+})/N(Ca^{2+})$ released from calcite and dolomite dissolution are 0:1 and 1:1, Equations (7) and (8) represent the chemical equations for the dissolution of calcite and dolomite. As shown in Figure 5c,d, most sampling points fall within the calcite dissolution zone ($N(Mg^{2+})/N(Ca^{2+})<0.4$), with no points distributed in the dolomite region ($N(Mg^{2+})/N(Ca^{2+})>0.6$). A few points are located in the mixed dissolution zone. This demonstrates that calcite is the main mineral component involved in carbonate dissolution in the area (Lin et al., 2018; Rupias, 2021), which is related to the lower solubility of dolomite compared to calcite.

$$CaCO_3(Calcite) + H_2CO_3 \rightarrow Ca^{2+} + 2H_2CO_3^- \quad (7)$$

$$CaMg(CO_3)_2(Dolomite) + 2H_2CO_3 \rightarrow Ca^{2+} + Mg^{2+} + 4HCO_3^- \quad (8)$$

Equations (9) shows the $N(Cl^-)/N(Na^+)$ ratio reflects the extent of Na^+ enrichment in groundwater, most water sample points plot below the y=x line, indicating that silicate dissolution and cation exchange are the primary sources of Na^+ (Figure 6a) (Rupias, 2021), and only few individual points

fall around the gypsum-mirabilite dissolution line, while the vast majority of samples are located above the y=x line (Figuere 6b), suggesting that sources other than gypsum and mirabilite significantly contribute to both Na^+ and Ca^{2+}. Equations (10) and (11) represent the chemical equations for the dissolution of mirabilite and gypsum. In the $N(SO_4^{2-})/N(Na^+)$ ratio diagram (Figure 6c), some points lie around the y=x line, while more points are above the line, indicating that mirabilite dissolution makes a notable contribution to SO_4^{2-} and Na^+, and that additional sources further elevate SO_4^{2-} levels. As shown in the $N(SO_4^{2-})/N(Ca^{2+})$ ratio plot (Figure 6d), all sample points are situated below the y = x line, demonstrating that Ca^{2+} originates from diverse sources, such as calcite dissolution.

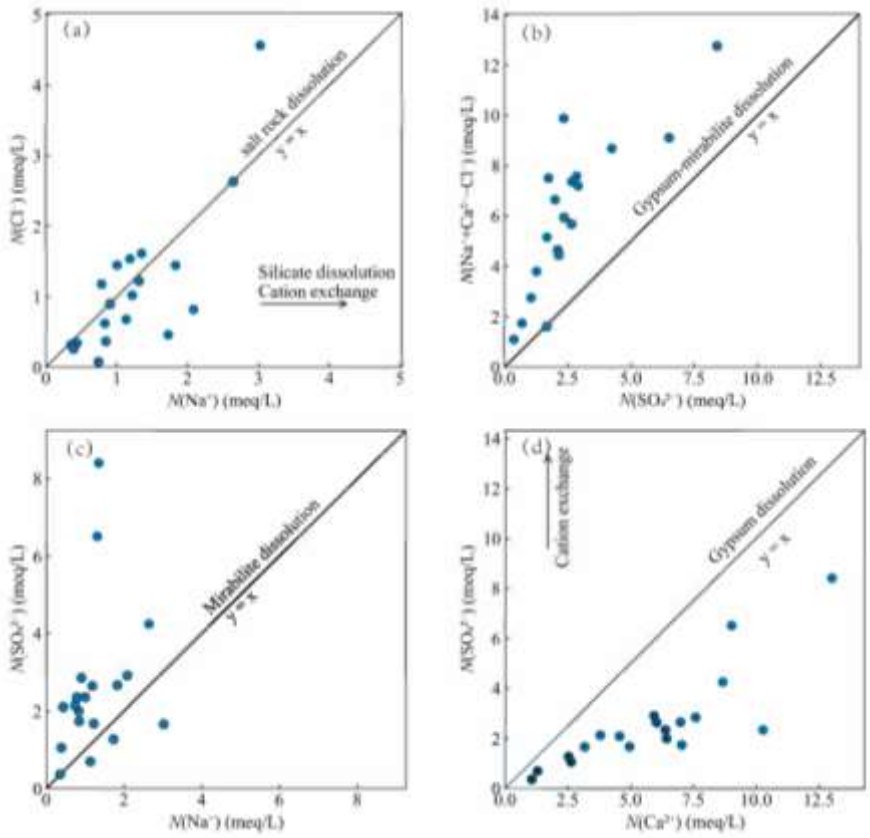


Figure.6 Scatter plots of (a) $N(Cl^-)$ VS. $N(Na^+)$; (b)$N(Na^+ + Ca^{2+} - Cl^-)$ VS. $N(SO_4^{2-})$; (c) $N(SO_4^{2-})$ VS. $N(Na^+)$; (d) $N(SO_4^{2-})$ VS. $N(Ca^{2+})$

$$NaCl \rightarrow Na^+ + Cl^- \quad (9)$$

$$Na_2SO_4 \cdot 10H_2O \rightarrow 2Na^+ + SO_4^{2-} + 10H_2O \quad (10)$$

$$CaSO_4 \cdot 2H_2O \Leftrightarrow Ca^{2+} + SO_4^{2-} + 2H_2O \quad (11)$$

3.4 Cation Exchange

Cation exchange is one of the key processes governing the formation of groundwater chemical composition. The ratio $N(Ca^{2+}+Mg^{2+}-SO_4^{2-}-HCO_3^-)$ / $N(Na^+ + K^+ - Cl^-)$ can be used to indicate the exchange between Ca^{2+}/Mg^{2+} and Na^+/K^+. When this ratio falls near the y=x reference line, it signifies the occurrence of cation exchange (Mclean et al., 2000; Fisher and Iii, 1997). Cation exchange was further analyzed using the Chloro-Alkaline Indices (CAI-I and CAI-II) (Schoeller,

1965). Furthermore, CAI-I and CAI-II can determine whether the cation exchange process is forward or reverse, these indices are calculated using Equations (12), (13), and the ion units are all meq/L.

$$CAI-I=(Cl^{-}-(Na^{+}+K^{+}))/Cl^{-} \quad (12)$$

$$CAI-II=(Cl^{-}-(Na^{+}+K^{+}))/(HCO_3^{-}+SO_4^{2-}+CO_3^{-}+NO_3^{-}) \quad (13)$$

As shown in Figure 7a, most data points cluster around the y=-x reference line, indicating significant cation exchange activity. The majority of points are located in the fourth quadrant where $N(Na^{+}+K^{+}-Cl^{-})>0$, suggesting direct cation exchange. In this process, Ca^{2+} and Mg^{2+} are adsorbed onto aquifer materials, while Na^{+} is released into the groundwater, leading to a decrease in Ca^{2+} and Mg^{2+} and an increase in Na^{+}. As illustrated in Figure 7b, most groundwater samples in the study area plot within the third quadrant (where both CAI-I and CAI-II are negative), providing further evidence for the prevalence of direct cation exchange.

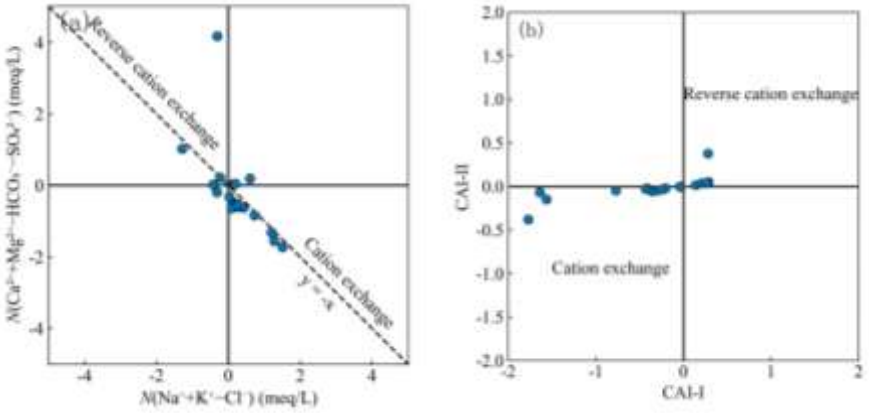


Figure.7 Cation exchange of groundwater and CAI distribution

3.5 Impact of Anthropogenic Activities

The ratios $N(Na^{+}+K^{+})/N(HCO_3^{-})$ and $N(Ca^{2+}+Mg^{2+})/N(HCO_3^{+})$ can reflect the relative contributions of carbonate/silicate dissolution and anthropogenic activities to groundwater composition (Deng et al., 2025; Yang et al., 2023). As shown in Figure 8a, most points are concentrated within the range of 0~2.5 on the x-axis and 0~2 on the y-axis. Samples are distributed along both the left-side line representing carbonates/silicates dissolution (y = 1-x) and the right-side line representing anthropogenic input (y =x-1). This indicates that anthropogenic activities, carbonates dissolution, and silicates dissolution collectively control the hydrochemical composition of groundwater in the study area. The excess $Na^{+}$and K^{+} primarily originate from anthropogenic inputs, confirming that human activities have a discernible influence on groundwater in the region.

NO_3^{-} is associated with industrial and mining activities, domestic wastewater discharge, and excessive agricultural fertilization. The relationship between $N(SO_4^{2-})/N(Ca^{2+})$ and $N(NO_3^{-})/N(Ca^{2+})$ can be used to analyze the impacts of industrial/mining activities, agricultural practices, and domestic sewage on groundwater chemistry (Han et al., 2023). Figure 8b reveals that the study area is more significantly affected by domestic sewage and agricultural activities. Combining this finding

with the spatial distribution of NO_3^- and land use types, elevated NO_3^- concentrations are predominantly found in urban and cultivated areas. This further substantiates that agricultural activities and domestic sewage are major contributors to NO_3^- in the groundwater system.

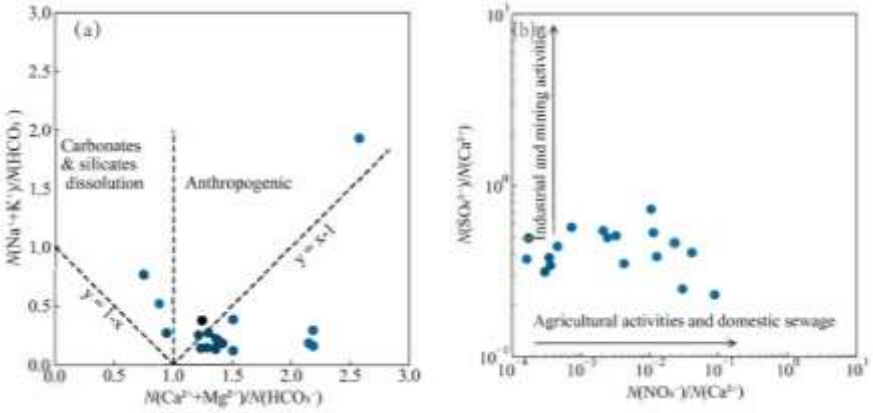


Figure.8 Scatter plots of (a) $N(Na^+ + K^+)/N(HCO_3^-)$ VS. $N(Ca^{2+} + Mg^{2+})/N(HCO_3^-)$; (b) $N(SO_4^{2-})/N(Ca^{2+})$ VS. $N(NO_3^-)/N(Ca^{2+})$

As shown in Figure 9a, most samples fall within the soil organic nitrogen and sewage input end-members, with some groundwater samples lying between the fertilizer input and soil organic nitrogen end-members. The study area encompasses the main urban zones of Meishan and Leshan cities, characterized by dense human populations and frequent activities, making sewage discharge a significant source of nitrogen in the region. Furthermore, as a key grain-producing area of the "Tianfu Granary", the study area generally has thick soil cover, which retains considerable residual nitrogen that subsequently enters groundwater in the form of soil organic nitrogen. Some points are distributed near the $c(NO_3^-)/c(Cl^-)$:$c(Cl^-)$ = 1:1 reference line but do not align clearly with a single end-member, indicating combined influences from agricultural fertilizers, soil organic nitrogen, and sewage (Li J et al., 2023; Li J et al., 2022). Although atmospheric precipitation can deliver NO_3^- to aquifers via rapid flow pathways, such pathways-common in karst regions-are not prevalent in the study area (Xie et al., 2025); therefore, atmospheric precipitation has minimal impact on nitrogen levels here.

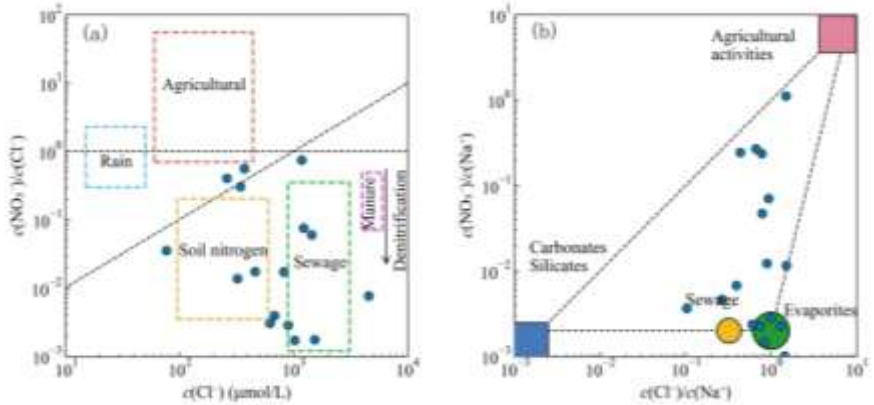


Figure.9 Scatter plots of (a) $c(NO_3^-)/c(Cl^-)$ VS. $c(Cl^-)$; (b) $c(Cl^-)/c(Na^+)$ VS. $c(NO_3^-)/c(Na^+)$

Additionally, one sampling point lies close to the indicator line for microbial denitrification. This

point exhibits the highest Cl^- and Na^+ concentrations and the second-highest K^+ concentration in the study area. Given that Cl^-, Na^+, and K^+ are indicative of domestic sewage and agricultural activities, and considering that this sampling well is the shallowest in the study area and thus most vulnerable to anthropogenic influence, it is inferred that surface-derived pollution (domestic or agricultural in origin) has led to salinization of the shallow groundwater. This pollution likely supplies organic carbon and creates an anaerobic environment, thereby driving denitrification processes. Overall, denitrification contributes only minimally to the natural microbial attenuation of NO_3^- in the study area.

Excessive human activities can elevate concentrations of Na^+, NO_3^-, and Cl^- in groundwater (Eslami et al., 2019; Xiao et al., 2016). By comparing the relationships among $c(NO_3^-)$, $c(Na^+)$, and $c(Cl^-)$, the extent of anthropogenic pollution in groundwater can be assessed (Fan et al. 2014). As shown in Figure 9b, most sampling points in the study area are located within the domains of domestic sewage, agricultural activities, and evaporite dissolution, corroborating earlier findings that domestic sewage and agricultural activities are major sources of NO_3^- recharge in the region. As a core area of the "Tianfu Granary" and a population-dense zone of Meishan and Leshan cities, anthropogenic activities-particularly agriculture and domestic sewage-exert a non-negligible influence on the shallow groundwater in this area.

3.6 Carbonates Dissolution Driven by Acidic Pollutants

Under natural conditions, $N(Ca^{2+}+Mg^{2+})$ derived from carbonates dissolution equals $N(HCO_3^-)$. When additional acidic substances participate in carbonate dissolution, an excess of $N(Ca^{2+}+Mg^{2+})$ occurs (Xie et al., 2025; Huang et al., 2017). As shown in Figure 10a,b, most sample points are located in the cation-excess region and distribute near the line $N(Ca^{2+}+Mg^{2+})/N(HCO_3^-+SO_4^{2-}+NO_3^-)=1$, indicating that acids other than carbonic acid contribute to carbonate dissolution in the study area. For a few points, $N(Ca^{2+}+Mg^{2+})/N(HCO_3^-+SO_4^{2-}+NO_3^-)<1$, suggesting that SO_4^{2-} and NO_3^- in groundwater are not solely derived from acidic pollutants and may originate from nitrogen -bearing organic matter or gypsum.

In Figure 10c, most sampling points plot between the carbonate-dissolution end-members dominated by carbonic acid and sulfuric acid, but are closer to the carbonic-acid-dominated end-member. This indicates that groundwater in the study area is primarily influenced by natural carbonate dissolution, although sulfuric acid also contributes significantly to the dissolution process. As illustrated in Figure 10d, a strong positive linear correlation ($R^2= 0.76$) exists between $N(SO_4^{2-}+NO_3^-)$ and $N(Ca^{2+}+Mg^{2+})$ in the groundwater, further confirming that carbonate dissolution is jointly controlled by carbonic acid and sulfuric acid.

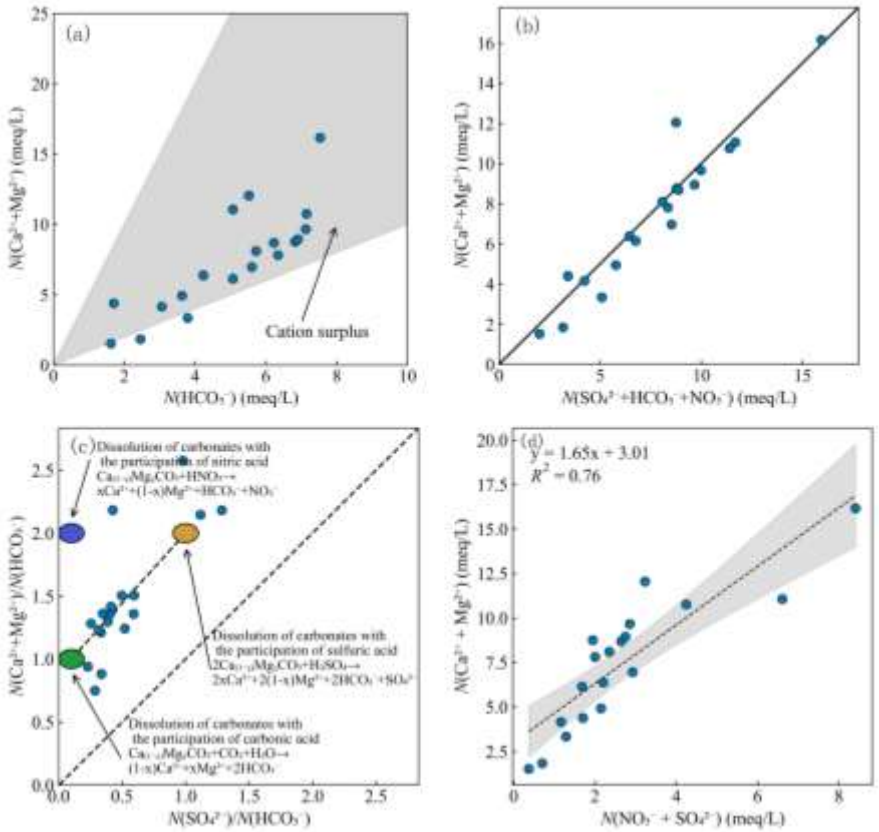


Figure.10 Control of carbonates dissolution by acidic pollutants in groundwater

3.7 Source Apportionment Based on PCA-APCS-MLR and PMF Models

The sample data met the basic requirements for multivariate statistical analysis, satisfying both the Kaiser-Meyer-Olkin (KMO) test (KMO > 0.50) and Bartlett's test of sphericity ($p = 0.00 < 0.05$). Principal Component Analysis (PCA) subsequently extracted four principal components (F1-F4) with eigenvalues greater than 1 after rotation, which collectively explained 84.76% of the total variance in the dataset. F1 explained the largest proportion of variance (47.15%) and exhibited high loadings on nearly all constituents except Mn^{2+} and NO_3^-, particularly on SO_4^{2-}, Ca^{2+}, Mg^{2+} and HCO_3^-. The variance explanation rates for F2, F3, and F4 were 12.96%, 12.77%, and 11.88%, respectively. These components were characterized by extremely high loadings (>0.85) on NO_3^-, NH_4^+ and Cl^-.

The APCS-MLR model was applied to quantify the contribution of each source represented by the principal components to the individual constituents. As shown in Table 4 and Figure 11a, F1 made significant contributions (ranging from 37.54% to 83.28%) to TH, SO_4^{2-}, Ca^{2+}, Mg^{2+}, K^+ and HCO_3^-. F2 contributed highly to NO_3^- and Mn^{2+}(44.33% and 68.60%, respectively). F3 was the primary contributor to NH_4^+ (15.54%), while F4 mainly contributed to Cl^- (48.92%). The contribution from unidentifiable sources was 25.40%.

The EPA PMF 5.0 software was employed to identify and quantify potential sources and their contributions. The model was run in "Robust" mode with 20 iterations. The number of factors was

increased incrementally from 2 to 6. The results indicated that the most stable solution with the minimum and most stable Q value was achieved with four factors, where the ratio of Q_{True}/Q_{Theo} was closest to 1. Furthermore, the coefficients of determination (r^2) for the modeled species ranged from 0.47 to 0.95 (Figure 11), and the scaled residuals for all samples fell within the range of -3~3. This demonstrates a satisfactory model fit to the observed data. As shown in Table 4 and Figure 11b, the average contributions of the four factors (F1-F4) were 46.44%, 21.88%, 18.67%, and 13.02%, respectively. F1 contributed significantly to multiple species, including TH, SO_4^{2-}, Ca^{2+}, Cl^-, Mg^{2+}, K^+ and HCO_3^-. F2 was responsible for 87.94% of NO_3^-. F3 was the dominant contributor to NH_4^+ (68.48%), and F4 primarily contributed to Cl^- (35.75%) and K^+ (64.05%). The factor profiles and contributions obtained from the APCS-MLR and PMF models were largely consistent.

Table 4. Source analysis contribution result matrix

Model	Parameter	F1	F2	F3	F4	Unknown
APCS-MLR	TH	83.28%	8.93%	1.05%	2.67%	4.07%
	SO_4^{2-}	72.63%	6.64%	2.75%	8.45%	9.53%
	Cl^-	25.18%	5.67%	0.79%	48.92%	19.44%
	Mn^{2+}	8.52%	68.60%	1.39%	2.69%	18.80%
	NH_4^+	21.53%	13.43%	15.54%	2.73%	46.76%
	NO_3^-	14.01%	44.33%	0.74%	3.41%	37.50%
	Ca^{2+}	81.01%	10.76%	1.24%	1.98%	5.01%
	Mg^{2+}	66.31%	0.92%	0.07%	4.67%	28.03%
	K^+	37.54%	8.65%	4.36%	7.90%	41.55%
	HCO_3^-	49.21%	3.04%	0.19%	4.26%	43.30%
Model	**Parameter**	**F1**	**F2**	**F3**	**F4**	
PMF	TH	24.02%	10.54%	61.35%	4.08%	-
	SO_4^{2-}	20.26%	9.35%	63.45%	6.94%	-
	Cl^-	7.61%	0.00%	56.64%	35.75%	-
	Mn^{2+}	0.00%	20.73%	79.27%	0.00%	-
	NH_4^+	9.05%	68.48%	22.47%	0.00%	-
	NO_3^-	87.94%	0.00%	3.19%	8.87%	-
	Ca^{2+}	22.30%	10.28%	64.25%	3.17%	-
	Mg^{2+}	26.04%	11.19%	55.42%	7.35%	-
	K^+	0.00%	35.95%	0.00%	64.05%	-
	HCO_3^-	21.55%	20.13%	58.32%	0.00%	-

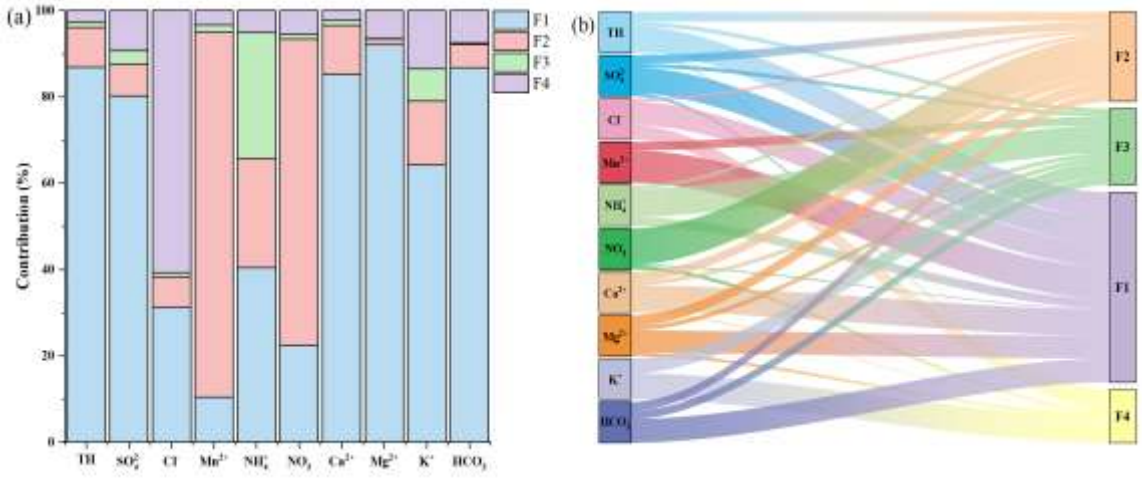


Figure.11 Source analysis result:(a)APCS-MLR; (b)PMF

F1 demonstrates significant contributions to TH, Ca^{2+}, Mg^{2+}, K^{+}, HCO_3^{-}, SO_4^{2-}. The weathering and dissolution of natural rocks and soils constitute the most fundamental and widespread source of these ionic components, primarily through the weathering and dissolution of carbonate and sulfate minerals. Carbonate minerals such as calcite ($CaCO_3$) and dolomite ($CaMg(CO_3)_2$) are key sources, directly releasing Ca^{2+}, Mg^{2+} and HCO_3^{-} upon dissolution. Associated potassium-bearing carbonate minerals (e.g., potassium feldspar) simultaneously release minor amounts of K^{+}. The dissolution of sulfate minerals like gypsum ($CaSO_4 \cdot 2H_2O$) and magnesium sulfate releases Ca^{2+}, Mg^{2+} and HCO_3^{-}. Therefore, F1 is interpreted as a natural geological source.

F2 shows high contributions to NO_3^{-} and Mn^{2+}. The enrichment of NO_3^{-} is typically associated with anthropogenic activities. Their co-occurrence in water bodies is mainly attributed to agricultural practices. The application of nitrogen-based fertilizers (e.g., urea, ammonium nitrate) leads to the leaching of related components into groundwater or their transport via runoff into surface water. Furthermore, agricultural tillage disrupts soil structure, causing originally immobilized manganese (e.g., MnO_2) to be reduced to soluble Mn^{2+} under anoxic conditions, which then migrates to water bodies. Industrial wastewater may contain both Mn^{2+} (e.g., from metal processing effluent) and NO_3^{-} (e.g., by-products of certain chemical processes). Untreated discharge can contaminate surface water and subsequently infiltrate groundwater. Waste materials like manganese-bearing slag and landfill leachate can also release Mn^{2+} under rainwater percolation, while the decomposition of organic matter or nitrogenous waste (e.g., plastics, food residues) in landfills can generate NO_3^{-}, jointly entering water bodies. Untreated domestic sewage contains nitrogenous organic matter (e.g., from detergents, excrement) that decomposes to produce NO_3^{-}. Manganese can also be introduced via pipe corrosion or manganese-containing materials in domestic waste. Through pipeline leakage or inadequate wastewater treatment, these contaminants can pollute surface and groundwater. In summary, F2 is considered a mixed source from industrial and agricultural activities.

F3 is characterized by its association with NH_4^{+}. In agricultural activities, nitrogenous fertilizers (e.g., ammonium bicarbonate) are a direct source of NH_4^{+}. The decomposition of organic fertilizers

(e.g., livestock manure, straw) also releases NH_4^+. Simultaneously, tillage-induced soil anoxia can inhibit nitrification, leading to NH_4^+ accumulation, which subsequently enters water bodies through leaching or runoff. Additionally, certain natural processes release NH_4^+, such as biological nitrogen fixation by microorganisms (e.g., rhizobia in legume root nodules, cyanobacteria) in soil or water, converting atmospheric N_2 into NH_4^+. Therefore, F3 is identified as reflecting agricultural influences under reducing environmental conditions.

F4 is closely associated with Cl^- and K^+. The use of detergents (e.g., laundry powders containing potassium chloride) and common salt (NaCl, often accompanied by minor K^+) in domestic wastewater introduces both Cl^- and K^+. Discharge of inadequately treated sewage or pipeline leakage leads to concurrent increases in Cl^- and K^+ concentrations in groundwater. Consequently, F4 is attributed to domestic sewage discharge.

3.8 Groundwater Quality Assessment Based on EWQI

This study utilized parameters with high detection frequencies and concentrations—including TDS, pH, K^+, Ca^{2+}, Na^+, Mg^{2+}, Cl^-, HCO_3^-, SO_4^{2-}, NO_3^-, NH_4^+, Mn^{2+}, Al^{3+}-for water quality evaluation. The Entropy-Weighted Water Quality Index (EWQI) was employed to determine the weights of these indicators in the study area. As shown in Table 5, aluminum (0.13), ammonia nitrogen (0.11), and manganese (0.09) are the primary controlling parameters, exhibiting relatively high weights and exerting a greater influence on water quality.

As illustrated in Figure 12, the EWQI scores range from 27.20 to 132.75, with an average score of 81.17. Groundwater quality in the study area can be classified into three categories: excellent, good, and medium. No samples were rated as poor or very poor. The respective proportions are 26.32%, 36.84%, and 36.84%. Overall, 63.16% of the water samples are suitable for direct human consumption.

Table 5. Weight of hydrochemical indicators

Parameter	Indicator				
Weight	pH	TH	TDS	SO_4^{2-}	Cl^-
	0.03	0.06	0.05	0.06	0.06
	Mn^{2+}	Al^{3+}	Na^+	NH_4^+	NO_3^-
	0.09	0.12	0.07	0.11	0.07
	Ca^{2+}	Mg^{2+}	K^+	HCO_3^-	
	0.06	0.06	0.07	0.08	

Note: The standard limit values for K, Ca^{2+}, Mg^{2+}, and HCO_3^- are based on the World Health Organization (WHO) recommended values, which are 20 mg/L, 200 mg/L, 150 mg/L, and 120 mg/L, respectively. The limit values for other indicators are all taken from GB/T 14848-2017 *Groundwater Quality Standard*.

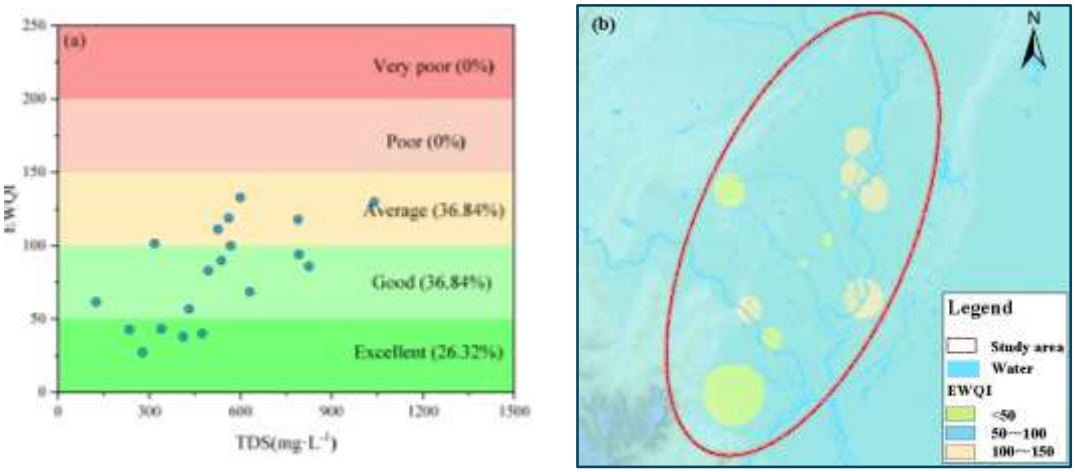


Figure.12 Grading visualization and spatial distribution of EWQI: (a) EWQI vs. TDS; (b) Spatial distribution of groundwater quality based on the EWQI ranks

3.9 Groundwater Health Risk Assessment

3.9.1 Health Risk Assessment from Groundwater Consumption

Following the USEPA evaluation framework and considering the exceedance hazards identified in the EWQI results, Mn^{2+} and NO_3^- were selected to assess the health risks posed via drinking water ingestion and dermal contact pathways. For this assessment, Mn^{2+} and NO_3^- are non-carcinogenic indicators. And there reference doses (RfD) are 0.14 mg/kg • d and 1.6 mg/kg • d, respectively.

As shown in Table 6, for children, the Mn^{2+} hazard indices range from 0 to 0.000574 (mean: 0.000259) for dermal contact and from 0 to 0.170776 (mean: 0.077042) for oral ingestion. Both are below the USEPA acceptable limit (risk index = 1). The NO_3^- hazard indices for children range from 0.001067 to 1.059589 (mean: 0.098453) for dermal contact and from 0.000458 to 0.454218 (mean: 0.042204) for oral ingestion, with the exception of one sampling point where the oral ingestion risk index exceeded 1(Figure 13a). All other values remain within the acceptable range.

For adults, the Mn^{2+} hazard quotients range from 0 to 0.000197 (mean: 0.000089) for dermal contact and from 0 to 0.073207 (mean: 0.031163) for oral ingestion, both below the acceptable limit. The NO_3^- hazard quotients for adults range from 0.000001 to 0.001220 (mean: 0.000113) for dermal contact and from 0.000458 to 0.454218 (mean: 0.042204) for oral ingestion, all within the acceptable range(Figure 13b).

In summary, nearly all risk indices are below 1, indicating generally good groundwater quality in the study area with low potential non-carcinogenic risk. However, the hazard indices for children are higher than the hazard quotients for adults, which may be attributed to children's lower body weight. One sampling point located near an urban area exhibited an HI value exceeding 1 (corresponding to NO_3^-N concentration of 54.6 mg/L), suggesting that children are more vulnerable than adults under similar exposure conditions. This finding highlights a point of concern for future drinking water safety management.

Table 6. Assessment results of health risks through drinking water intake and dermal contact

Parameter	Exposure route	Risk in Adults			Risk in Children		
		Minimum	Maximum	Average	Minimum	Maximum	Average
Mn^{2+}	Der	0	1.97×10^{-4}	8.87×10^{-5}	0	5.74×10^{-4}	2.59×10^{-4}
	Oral	0	7.32×10^{-2}	3.12×10^{-2}	0	0.171	0.0770
	Comprehensive	0	7.34×10^{-2}	3.31×10^{-2}	0	0.171	0.0773
NO_3^-	Der	1.23×10^{-6}	1.22×10^{-3}	1.13×10^{-4}	3.58×10^{-6}	3.56×10^{-3}	3.31×10^{-4}
	Oral	4.58×10^{-4}	0.454	4.22×10^{-2}	1.07×10^{-3}	1.06	0.0985
	Comprehensive	4.59×10^{-4}	0.455	4.23×10^{-2}	1.07×10^{-3}	1.06	0.0988
Total risk	Der	0	7.70×10^{-4}	3.47×10^{-4}	9.29×10^{-5}	3.63×10^{-3}	5.89×10^{-4}
	Oral	0	0.244	0.11	0.0277	1.08	0.175
	Comprehensive	0	0.245	0.11	0.0277	1.08	0.176

Note: The total risk value is obtained by adding the risk values induced by Mn^{2+} and NO_3^- under different exposure routes.

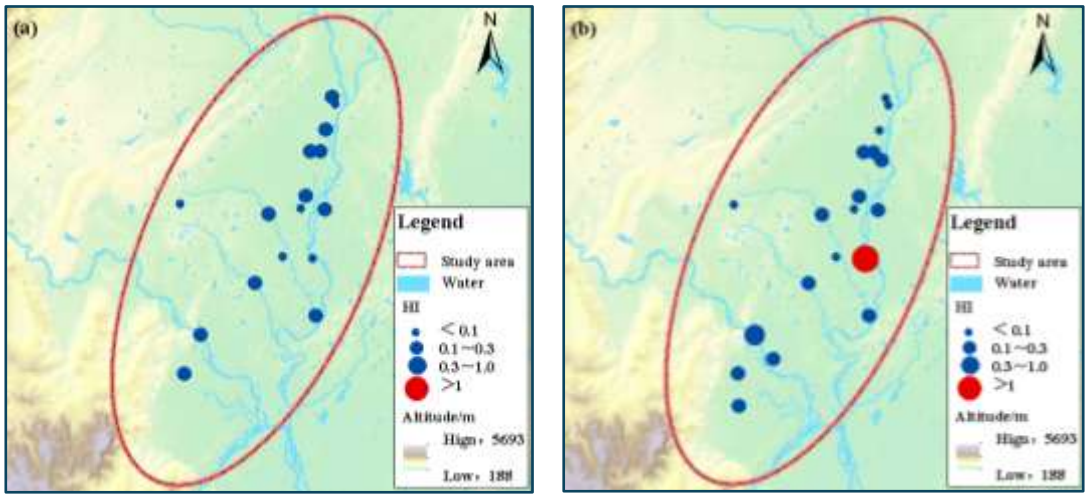


Figure.13 Spatial distrbution of non-carcnogenie health risks: (a) Risk in Adults; (b) Risk in Children

3.9.2 Assessment of Groundwater Suitability for Irrigation

As a core area of the "Tianfu Granary," the study region plays a critical role in ensuring food security. The chemical composition of irrigation water significantly influences farmland soil properties and fertility. According to the GB 5084-2021 *Standards for Irrigation Water Quality*, only one location in the study area, with a high TDS value (1040 mg/L), is deemed unsuitable for irrigation (Figure 14a). Groundwater from all other sampling points is suitable for irrigation, indicating generally good overall water quality, with only isolated samples potentially affected by geological background conditions or anthropogenic activities.

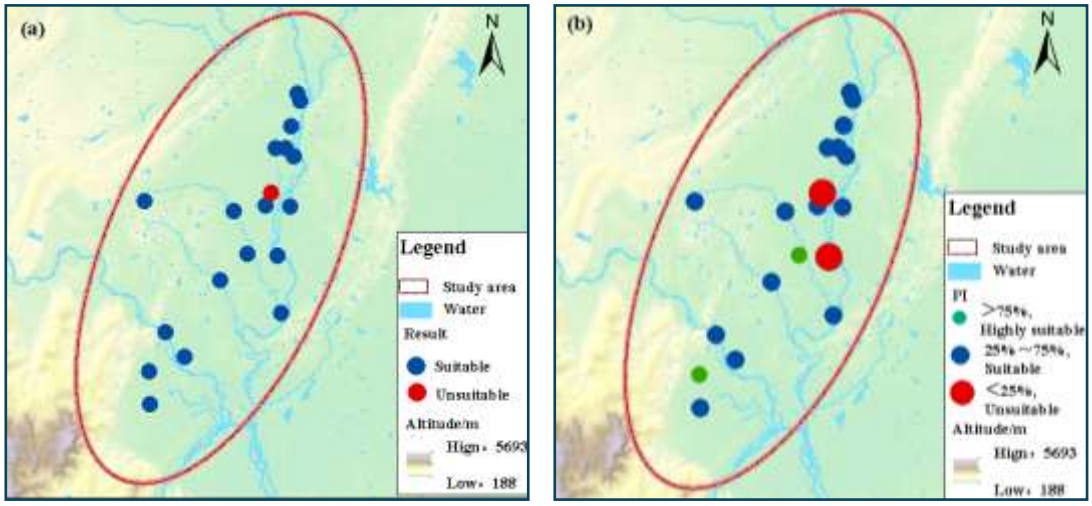


Figure.14 Spatial distrbution of groundwater irrigation water quality: (a) GB5084-2021 *Irrigation Water Quality Standards*; (b) PI

As presented in Table 7, the groundwater's suitability for irrigation was analyzed using an evaluation index system including SAR, MH, Na%, PI, and RSC, based on the milliequivalent concentrations of K^+, Ca^{2+}, Na^+, Mg^{2+} and HCO_3^-. With the exception of a few points characterized by high Ca^{2+} content being classified as unsuitable under the PI index system (Figure 14b), the overall water quality is good and suitable for irrigation use.

Table 7. Results of irrigation quality assessment of groundwater

Parameter	Value	Classification	No./%	Parameter	Value	Classification	No./%
SAR	<10	Excellent	19/100%	MH(%)	<50	Suitable	19/100%
	10~18	Good	0				
	18~26	Moderately suitable	0		>50	Not suitable	0
	>26	Unsuitable	0				
Na%	<20	Excellent	15/78.95%	PI(%)	>75	Highly suitable	2/10.53%
	20~40	Good	4/21.05%		25~75	Suitable	15/78.94%
	40~80	Moderately suitable	0		<25	Unsuitable	2/10.53%
	>80	Unsuitable	0				
SC(%)	<20	Highly suitable	13/68.42%	RSC	<1.25	Highly suitable	7
	20~40	Moderately suitable	4/21.05%		1.25~2.5	Suitable	12
	40~60	Suitable	2/10.53%		>2.5	Unsuitable	0
	60~80	Uncertain	0				
	>80	Unsuitable	0				

The Electrical Conductivity (EC) of groundwater in the study area ranges from 155~717.81 μS/cm. According to the United States Salinity Laboratory (USSL) irrigation water classification diagram (K TD, 1959), all groundwater samples fall within the S1 zone (low SAR, medium to low salinity) (Figure 15.a). Furthermore, the Wilcox diagram(Figure 15.b), which relates salinity and sodium percentage, also indicates that the groundwater in the study area is highly suitable for

irrigation (Wilcox, 2002).

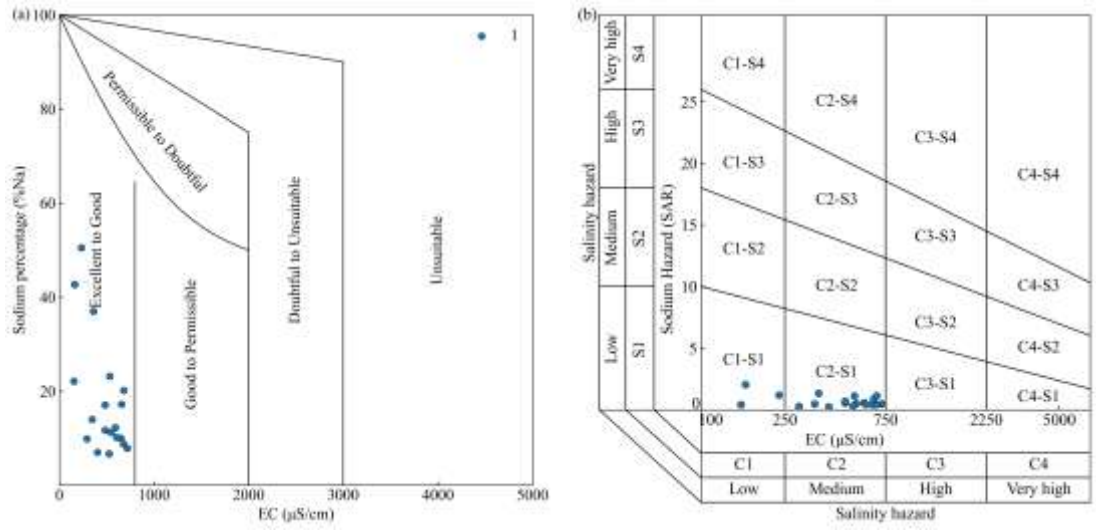


Figure.15 Scatter plots of (a) USSL;(b)Wilcox

In summary, only one sampling location was identified as unsuitable for irrigation water use under both the GB 5084-2021 *Standards for Irrigation Water Quality* and the PI (Permeability Index) evaluation system. Another location was found unsuitable for irrigation and also posed potential health risks to children. Both sites are situated in the upstream and downstream areas of the main urban zone of Meishan City, which may be attributed to localized degradation of groundwater quality due to anthropogenic activities. Overall, groundwater quality in the study area is generally good.

4 Conclusion

(1) The pH of the Quaternary porous water in the study area ranges from 6.33 to 7.71 (average: 7.04), indicating a predominantly neutral condition. The total dissolved solids (TDS) range from 125 to 1040 mg/L (average: 525.05 mg/L). The average cation concentrations follow the order: Ca^{2+} (117.54 mg/L) > Na^{+} (28.86 mg/L) > Mg^{2+} (19.32 mg/L) > K^{+} (4.61 mg/L), with Ca^{2+} concentrations ranging from 21.4 to 261 mg/L. The dominant anion is HCO_3^{-}, with concentrations between 99.2 and 459.4 mg/L (average: 307.03 mg/L). The primary hydrochemical type is Ca-HCO_3. According to the GB/T 14848-2017 *Groundwater Quality Standard*, the main indicators exceeding the standard limits are Mn^{2+} (73.68%) and total hardness (TH) (31.58%). Exceedances were also observed for SO_4^{2-} (10.53%), TDS (5.26%), pH (5.26%), and NO_3^{-}-N (5.26%).

(2) Gibbs diagrams indicate that the hydrochemistry of the unconsolidated porous water in the Emei-Jiajiang Plain is primarily controlled by rock weathering. The dissolution of carbonates and silicates is the key to the hydrochemical formation of the unconsolidated porous water in Emei-Jiajiang Plain, with calcite being the main mineral component involved in carbonate dissolution. Mirabilite dissolution contributes significantly to SO_4^{2-} and Na^{+}. Positive cation exchange occurs in the study area, where Ca^{2+} and Mg^{2+} are adsorbed by the aquifer materials. Groundwater chemistry is dominated by natural carbonate dissolution, with sulfuric acid also participating significantly in

the process. Anthropogenic activities have a discernible impact on groundwater in the study area, with agricultural practices and domestic sewage being major contributors to NO_3^-. The agricultural influence is primarily manifested through the thick soil cover retaining substantial residual nitrogen, which enters groundwater as soil organic nitrogen. Denitrification plays a minor role in the natural microbial attenuation of NO_3^- in the region.

(3) Results from both APCS-MLR and PMF models indicate that natural sources (F1), mixed industrial and agricultural sources (F2), agricultural activities (F3), and domestic sewage (F4) are the main factors influencing groundwater in the study area. F1 contributes significantly to TH, Ca^{2+}, Mg^{2+}, K^+, HCO_3^-, and SO_4^{2-}, with weathering and dissolution of natural rocks and soils being the most fundamental and widespread source of these ions. F2 shows high contributions to NO_3^- and Mn^{2+}. The enrichment of NO_3^- is typically related to human activities, and industrial wastewater may contain both Mn^{2+} and NO_3^-. F3 is characterized by NH_4^+, with nitrogenous fertilizers in agriculture being a direct source. F4 is closely associated with Cl^- and K^+, being attributed to domestic sewage discharge.

(4) The EWQI evaluation results show that Al^{3+} (weight: 0.13), NH_4^+ (0.11), and Mn^{2+} (0.09) are the primary controlling factors. The average EWQI score is 81.17, with 63.16% of the water samples suitable for direct human consumption. The health risk indices for nearly all sampling points are below 1, indicating low potential non-carcinogenic risk. However, one point exhibited an $HI_{N,oral}$, oral value exceeding 1, posing a potential health risk to children. Based on multiple irrigation suitability evaluation methods, groundwater in the study area is generally suitable for irrigation, though only a few exceptions.

(5) Due to the constraints of the project deployment, this study is limited to only 19 groundwater samples and lacks isotopic data. These limitations introduce some uncertainty to the findings, which will be addressed in subsequent research.

Declarations

Author Contributions: H.L.(Hao Liu): conceptualization, methodology, software, validation, formal analysis, investigation, resources, data curation, writing—original draft preparation, writing—review and editing, visualization, supervision, project administration, funding acquisition; X.H.(Xin Huang): methodology, software, validation, investigation, resources, data curation, writing—original draft preparation, writing—review and editing, visualization; A.B.H.: methodology, formal analysis, investigation, resources, data curation, writing—original draft preparation; J.B.S(Ji Bo Shi): methodology, formal analysis, investigation, resources, data curation, writing—original draft preparation; Y.M.L.(Yan Ming Liu): conceptualization, methodology, software, validation,formal analysis, ;investigation, resources, data curation, writing—original draft preparation, writing—review and editing, visualization, supervision, project administration, funding acquisition. P.Z.(Peng Zhang): conceptualization, methodology, software, validation, formal analysis, investigation, resources, data curation, writing—original draft preparation, writing—

review and editing. All authors have read and agreed to the published version of the manuscript. All authors have read and agreed to the published version of the manuscript.

Funding: This research is funded by “Ministry of Natural Resources Provincial Collaboration Projects, grant number 2024ZRBSHZ021” .

Data Availability Statement: The original contributions presented in this study are included in the article.

Conflicts of Interest: The authors declare no conflicts of interest.

References

Arumugam K., Elangovan K. 2009. Hydrochemical characteristics and groundwater quality assessment in Tirupur Region, Coimbatore District, Tamil Nadu, India. Environ Geol 58, 1509-1520. DOI: https://doi.org/10.1007/s00254-008-1652-y.

Bian, Jianmin, Nie, Wang R, et al. 2018. Hydrochemical characteristics and quality assessment of groundwater for irrigation use in central and eastern Songnen Plain, Northeast China. Environmental Monitoring & Assessment An International Journal.

Bishwakarma K, Wang GX, Zhang F, et al. 2022. Hydrochemical characterization and irrigation suitability of the Ganges Brahmaputra River System: review and assessment. Journal of Mountain Science, 19(2): 388-402. DOI: https://doi.org/10.1007/s11629-021-6834-z.

Chen JS, Zhou JL, Wei X, et al. 2020. Spatial distribution and influencing factors of "three-nitrogen" of groundwater in the plain of Kashgar River basin, Xinjiang.Environmental Chemistry, 39(11): 3246-3254. (in Chinese) DOI: https://doi.org/10.7524/j.issn.0254-6108.2019081904.

Chin, Yik, Lin, et al. 2012. Delineation of temporal variability and governing factors influencing the spatial variability of shallow groundwater chemistry in a tropical sedimentary island, Journal of Hydrology, 432–433(1):26-42. DOI: https://doi.org/10.1016/j.jhydrol.2012.02.015.

Cui JQ, Li XY, Shi HB, et al. 2020. Chemical evolution and formation mechanism of groundwater in Hetao Irrigation Area. Environmental Science, 41(9):10. (in Chinese) DOI: https://doi.org/10.13227/j.hjkx.202003150.

Deng XY, Jian K, Qi YF, et al.2025. Hydrochemical characteristics of groundwater and its formation mechanism in area along the Yellow River in Henan Province. Water Resources Protection, 41(04):135-143. (in Chinese)

Doneen LD. 1964. Notes on Water Quality in Agriculture.// Water Science and Engineering Paper 4001. Davis: University of California.

Du XQ, Fang M, Ye XY. 2018. Research progress on the sources of inorganic nitrogen pollution in groundwater and identification methods. Environmental Science, 39(11):10. (in Chinese) DOI: https://doi.org/10.13227/j.hjkx.201802088.

Eaton, Frank M. 1950. Significance of Carbonates in Irrigation Waters. Soil Sci, 69, 123-134. DOI: https://doi.org/10.1097/00010694-195002000-00004.

Eslami F, Yaghmaeian K, Mohammadi A, et al.2019. An integrated evaluation of groundwater quality using drinking water quality indices and hydrochemical characteristics: a case study in Jiroft, Iran.Environmental Geology, 78(10):314.1-314.10. DOI: https://doi.org/10.1007/s12665-019-8321-1.

Esmaeili-Vardanjani M, Rasa I, Amiri V, et al. 2015. Evaluation of groundwater quality and assessment of scaling potential and corrosiveness of water samples in Kadkan aquifer,

Khorasan-e-Razavi Province, Iran. Environmental Monitoring and Assessment, 187(2):53.DOI: https://doi.org/10.1007/s10661-014-4261-0.

Fan BL, Zhao ZQ, Tao FX ,et al. 2014. Characteristics of carbonate, evaporite and silicate weathering in Huanghe River basin: A comparison among the upstream, midstream and downstream. Journal of Asian Earth Sciences, 96(dec.15):17-26. DOI: https://doi.org/10.1016/j.jseaes.2014.09.005.

Fisher R S, Iii W F M. 1997. Hydrochemical evolution of sodium-sulfate and sodium-chloride groundwater beneath the Northern Chihuahuan Desert, Trans-Pecos, Texas, USA. Hydrogeology Journal, 5(2):4-16. DOI: https://doi.org/10.1007/s100400050102.

Gaillardet J , Dupre B , Louvat P ,et al. 1999. Global silicate weathering and CO"2 consumption rates deduced from the chemistry of large river.CHEMICAL GEOLOGY, 159(1):3-30. DOI: https://doi.org/10.1016/S0009-2541(99)00031-5.

Gao YY. 2020. Spatio-Temporal evolution of hydrochemical components and human health risk assessment of groundwater in Guanzhong Plain. Chang'an University. DOI: https://doi.org/10.26976/d.cnki.gchau.2020.000029.

Gibbs R J. 1970. Mechanisms Controlling World Water Chemistry.Science, 170[2025-10-15]. DOI: https://doi.org/10.1126/science.170.3962.1088.

Han SB, Zhou XZ, Zheng Yan, et al. 2023. Formation mechanism and source apportionment of hydrochemical components in groundwater in the Yinchuan Plain. Environmental Science, 45(08):4577-4588. (in Chinese) DOI: https://doi.org/10.13227/j.hjkx.202308211.

Huang QB, Qin XQ, Liu PY, et al. 2017. Impact of sulfuric and nitric acids on carbonate dissolution, and the associated deficit of CO2 uptake in the upper-middle reaches of the Wujiang River, China.Journal of Contaminant Hydrology, 203(aug.):18-27.DOI: https://doi.org/10.1016/j.jconhyd.2017.05.006.

K H B. 1969. Description and classification of media for hydrogeochemical investigations // Symposium on ground water studies in arid and semiarid regions .

K TD. 1959. Groundwater hydrology. New York: Wiley .

Li J , Zhu D , Zhang S ,et al. 2022. Application of the hydrochemistry, stable isotopes and MixSIAR model to identify nitrate sources and transformations in surface water and groundwater of an intensive agricultural karst wetland in Guilin, China. Ecotoxicology and Environmental Safety, 231:113205-. DOI: https://doi.org/10.1016/j.ecoenv.2022.113205.

Li J, Zou S, Wang J, et al. 2023. Spatiotemporal variability and control factors of NO.Chemosphere, 313:137435.DOI: https://doi.org/10.1016/j.chemosphere.2022.137435.

Li L. 2021. Characteristics and genesis of Quaternary sediments from Longmendong River and Emei River in Emei Plain. Chengdu University of Technology. DOI: https://doi.org/10.26986/d.cnki.gcdlc.2021.000949.(in Chinese)

Lin YS, Pei JG, ZOU SZ,et al. 2018. Red bed karst and its hydrochemical characteristics of groundwater in the downstream of Qingjiang River,China. Journal of Guangxi Normal University:Natural Science Edition, 36(3):8. (in Chinese) DOI: https://doi.org/10.16088/j.issn.1001-6600.2018.03.017.

Liu N, Chen M, Gao DD, et al. 2024 .Hydrochemical characteristics and health risk assessment of shallow groundwater in the plain zone of Deyang City. Environmental Science, 45(4):2129-2141. (in Chinese) DOI: https://doi.org/10.13227/j.hjkx.202305110.

Liu Y, Zheng BH, Fu Q, et al. 2013. Application of water pollution index method in river water quality assessment. Environmental Monitoring, 29(3): 49-55. (in Chinese). DOI: https://doi.org/10.3969/j.issn.1000-7709.2010.08.010.

693 Lu HY, Hu ZY, Zhang RJ, et al. 2010. Spatial variability of nitrogen in soils in farmland adjacent
694 suburban villages at northern bank of Dianchi Lake. Journal of Agro-Environment Science,
695 29(8):6. (in Chinese) DOI: https://doi.org/CNKI:SUN:NHBH.0.2010-08-033.

696 Lv XL, Liu JT, Zhou B et al. 2019.Distribution and source of nitrogen pollution in groundwater in
697 the Tacheng Basin. Hydrogeology & Engineering Geology, (2):9. (in Chinese) DOI:
698 https://doi.org/CNKI:SUN:SWDG.0.2019-02-007.

699 Mclean W, Jankowski J, Lavitt N. 2000. Groundwater quality and sustainability in an alluvial aquifer,
700 Australia.

701 Ministry of Ecology and Environment of the People's Republic of China, & Standardization
702 Administration of China. (2017). GB 14848-2017, Standard for groundwater quality.

703 Na Bahrami M., Zarei A.R., Rostami F. 2020. Temporal and spatial assessment of groundwater
704 contamination with nitrate by nitrate pollution index (NPI) and GIS (case study: Fasarud Plain,
705 southern Iran). Environ Geochem Health 42, 3119-3130. DOI: https://doi.org/10.1007/s10653-
706 020-00546-x.

707 Paatero P, Tapper U. 1994. Positive matrix factorization: A non-negative factor model with optimal
708 utilization of error estimates of data values. Environmetrics, 5(2). DOI:
709 https://doi.org/10.1002/env.3170050203.

710 Richards L.A. 1954. Diagnosis and Improvement of Saline and Alkali Soils. Soil Science, 64:290.
711 DOI: https://doi.org/10.1097/00010694-194711000-00013.

712 Rupias O J B, Pereira S, Abreu A E S D. 2021.Hydrogeochemistry and groundwater quality
713 assessment using the Water Quality Index and Heavy-metal Pollution Index in the alluvial plain
714 of Atibaia River- Campinas/SP, Brazil. Groundwater for Sustainable Development. DOI:
715 https://doi.org/10.1016/j.gsd.2021.100661.

716 Schoeller H. 1965. Hydrodynamique dans le karst(Hydrodynamics of the karst)//Proceedings of
717 the Hydrology of Fractured Rocks.Paris.UNESC0.1965 .3 -20.

718 Shrestha S, Kafle R, Pandey V P. 2016. Evaluation of index-overlay methods for groundwater
719 vulnerability and risk assessment in Kathmandu Valley, Nepal.Science of the Total
720 Environment, 779. DOI: https://doi.org/10.1016/j.scitotenv.2016.09.141.

721 Tang JP, Zhang Q, Hu Y, et al. 2019. Groundwater chemical characteristics and analysis of their
722 controlling factors in an alluvial fan of Jianjiang River. Environmental Science, 40(7):10. (in
723 Chinese). DOI: https://doi.org/10.13227/j.hjkx.201901006.

724 Thurston G D, Spengler J D. 1987. A quantitative assessment of source contributions to inhalable
725 particulate matter pollution in metropolitan Boston. Atmospheric Environment, 19(1):9-25.
726 DOI: https://doi.org/10.1016/0004-6981(85)90132-5.

727 Todd, D.K.; Mays, L.W. 1980. Groundwater Hydrology, 2nd ed.; John Wiley & Sons: Hoboken, NJ,
728 USA.

729 USEPA. 2004. Risk Assessment Guidance for Superfund Volume I: Human Health Evaluation
730 Muanual (Part e, supplemental guidance for dermal risk assessment) final.

731 Wilcox L V .2002. Classification and use of irrigation waters.Glycobiology, 12(3):229-234(6). DOI:
732 10.1093/glycob/12.3.229.

733 Xiao J, Jin, Z.D., Zhang ZD, F. 2016. Spatial characteristics and controlling factors of chemical
734 weathering of loess in the dry season in the middle Loess Plateau, China. Hydrological
735 Processes, DOI: https://doi.org/10.1002/hyp.10959.

736 Xie H, Shen H Y, Zhang HD, et al. 2025. Distributions and driving factors of hydrochemical
737 compositions in different types of karst groundwater in Qingjiang River Basin. Environmental
738 Science, 46(03):1417-1426. (in Chinese) DOI: https://doi.org/10.13227/j.hjkx.202401091.

739 Xu B, Zhang Y. 2018. Contamination characteristics and human health risk assessment of nitrate in
740 shallow groundwater at Jinghui irrigation district in Shaanxi province,China. Journal of Arid
741 Land Resources and Environment. 32(7):6. (in Chinese) DOI:
742 https://doi.org/CNKI:SUN:GHZH.0.2018-07-011.

743 Xu JP, Xu JP. 2001. Application of WPI index in surface water environmental quality assessmen.
744 Environmental Monitoring in China, (1): 47-49.(in Chinese) DOI:
745 https://doi.org/10.3969/j.issn.1002-6002.2001.01.016.

746 Yang YL, Jin J, Qi X, et al. 2023. Hydrochemical characteristics and formation mechanism analysis
747 of shallow groundwater in the northern hilly region of Ganzhou. Geological Survey of China,
748 10(06):60-68. (in Chinese) DOI: https://doi.org/10.19388/j.zgdzdc.2023.06.07.

749 Zhai Y, Zheng F, Zhao X, et al. 2019. Identification of hydrochemical genesis and screening of
750 typical groundwater pollutants impacting human health: A case study in Northeast China.
751 Environmental Pollution, 252(Pt B). DOI: https://doi.org/10.1016/j.envpol.2019.05.158.

752 Zhang H, Li QL, Guo SS, et al. 2019. Spatial-temporal heterogeneity and pollution sources of
753 groundwater pollution in typical area of Chengdu Plain. Acta Scientiae Circumstantiae,
754 39(10):12. (in Chinese) DOI: https://doi.org/CNKI:SUN:HJXX.0.2019-10-041.

755 Zhang J, Su CL, Zhang C, et al. 2010. Comprehensive index based entropy and weight for
756 groundwater quality evaluation. Water Resources and Power, 28(08): 30-32. (in Chinese). DOI:
757 https://doi.org/10.3969/j.issn.1000-7709.2010.08.010.

758 Zhang QD, Yang RB, Liu ZN, et al. 2020. Characteristics of hydrogeochemistry and isotope in the
759 Zhefang area of western Yunnan,China. Journal of Chengdu University of Technology: Science
760 & Technology Edition, 47(5):13. (in Chinese) DOI: https://doi.org/10.3969/j.issn.1671-
761 9727.2020.05.10.

762 Zhang Y , Xu B , Guo Z ,et al. 2019. Human health risk assessment of groundwater arsenic
763 contamination in Jinghui irrigation district, China. Journal of Environmental Management,
764 237:163-169.DOI: https://doi.org/10.1016/j.jenvman.2019.02.067.

765 Zhou XL. 1981. Hydrogeological survey report of Emei area H-48-20, Sichuan Province, Scale
766 1:200,000. Sichuan Provincial Bureau of Geology and Mineral Exploration and Development,
767 Hydrogeology Team.

768 Zhu DN, Zhou SZ, Li J, et al. 2021. Pollution and irrigation applicability of surface water from
769 wet,normal,and dry periods in the Huixian Karst Wetland,China. Environmental Science,
770 42(05):2240-2250. (in Chinese) .DOI: https://doi.org/10.13227/j.hjkx.202010087.